Published in final edited form as:
J Hepatol. 2013 November ; 59(5): 999–1006. doi:10.1016/j.jhep.2013.07.010.

Systemically delivered measles virus-infected mesenchymal stem cells can evade host immunity to inhibit liver cancer growth

Hooi-Tin Ong[1], **Mark J. Federspiel**[2], **Chang M. Guo**[3], **London Lucien Ooi**[4], **Stephen J. Russell**[5], **Kah-Whye Peng**[5], and **Kam M. Hui**[1,6,7,8,*]

[1]Bek Chai Heah Laboratory of Cancer Genomics, Humphrey Oei Institute of Cancer Research, Singapore

[2]Toxicology and Pharmacology Laboratory, Mayo Clinic, Rochester, MN, USA

[3]Department of Orthopedic, Singapore General Hospital, Singapore

[4]Division of Surgical Oncology, Singapore General Hospital, Singapore

[5]Department of Molecular Medicine, Mayo Clinic, Rochester, MN, USA

[6]Cancer and Stem Cell Biology Program, Duke-NUS Graduate Medical School, Singapore

[7]Department of Biochemistry, Yong Loo Lin School of Medicine, National University of Singapore, Singapore

[8]The Institute of Molecular and Cell Biology, A*STAR, Biopolis Drive Proteos, Singapore

Abstract

Background & Aims—Although attenuated measles virus (MV) has demonstrated potent oncolytic activities towards human cancers, it has not yet been widely adopted into clinical practice. One of the major hurdles is the presence of pre-existing anti-MV immunity in the recipients. In this study, we have evaluated the combination of the potent oncolytic activity of the attenuated MV with the unique immunoprivileged and tumor-tropic biological properties of human bone marrow-derived mesenchymal stem cells (BM-hMSCs) to combat human hepatocellular carcinoma (HCC), orthotopically implanted in SCID mice, passively immunized with human neutralizing antibodies against MV as a preclinical model.

Methods—SCID mice were orthotopically implanted with patient-derived HCC tissues and established HCC cell lines. SCID mice were passively immunized with human neutralizing anti-measles antibodies. Bioluminescence and fluorescence imaging were employed to monitor the

*Corresponding author. Address: Division of Cellular and Molecular Research, National Cancer Centre, 11 Hospital Drive, Singapore 169610, Singapore. Tel.: +65 6436 8338; fax: +65 6226 3843. cmrhkm@nccs.com.sg (K.M. Hui).

Supplementary data

Supplementary data associated with this article can be found, in the online version, at http://dx.doi.org/10.1016/j.jhep.2013.07.010.

Conflict of interest

The authors who have taken part in this study declared that they do not have anything to disclose regarding funding or conflict of interest with respect to this manuscript.

ability of systemically delivered MV-infected BM-hMSCs to infiltrate the implanted tumors and their effects on tumor growth.

Results—Systemically delivered MV-infected BM-hMSCs homed to the HCC tumors implanted orthotopically in the liver and it was evidenced that BM-hMSCs could transfer MV infectivity to HCC via heterofusion. Furthermore, therapy with MV-infected BM-hMSCs resulted in significant inhibition of tumor growth in both measles antibody-naïve and passively-immunized SCID mice. By contrast, when cell-free MV viruses were delivered systemically, antitumor activity was evident only in measles antibody-naïve SCID mice.

Conclusions—MV-infected BM-hMSCs cell delivery system provides a feasible strategy to elude the presence of immunity against MV in most of the potential cancer patients to be treated with the oncolytic MV viruses.

Keywords

Systemic virotherapy; Oncolytic measles virus; Hepatocellular carcinoma; Orthotopically implanted HCC tumor model; Mesenchymal stem cells as cell delivery vehicles; Human neutralizing antibody

Introduction

Hepatocellular carcinoma (HCC) is one of the most common malignancies worldwide and is the third leading cause of cancer-related deaths [1–3]. Liver transplantation (LT) offers one of the best treatments for HCC since it removes both the tumor and the underlying liver disease [4,5]. Unfortunately, the need to obtain the optimal benefit from the limited number of organs available has prompted the selection of those patients with early HCC for LT and has unavoidably led to many controversies around the use of LT in HCC patients [6]. Surgery currently offers the only possibility of prolonged survival in HCC patients. Unfortunately, recurrence occurs in more than two-thirds of these patients despite initial curative intent and converts the situation to a dismal prognosis. Transcatheter arterial chemoembolization (TACE) is also a treatment option for patients with preserved liver function and HCC confined to the liver [7]. However, the survival benefit of conventional TACE is modest. Despite the successful approval of sorafenib and the fact that its clinical applications have shown good tolerability in the studied populations [8,9], the prognosis for patients with advanced hepatocellular carcinoma (HCC) is poor and systemic therapies for advanced HCC remains an unmet medical need among patients with HCC.

Oncolytic virotherapy is an emerging treatment modality that uses replication-competent viruses to destroy cancers [10]. Oncolytic viruses are viruses that selectively infect or replicate in cancer cells but without causing harm to normal tissues and thus make them potentially therapeutically useful. Many naturally occurring viruses, including some naturally attenuated viral strains, have a preferential, although non-exclusive, tropism for tumors and tumor cells. Others are genetically modified to mediate oncolytic effects. In addition to the killing of infected cells, oncolytic viruses can mediate the killing of uninfected cancer cells by indirect mechanisms such as destruction of tumor blood vessels,

amplification of specific anticancer immune responses or through specific activities of transgene-encoded proteins expressed from engineered viruses [10].

The attenuated Edmonston vaccine strain of measles virus (MV) has demonstrated potent selective oncolytic activity against a number of human cancers, including HCC [11,12]. MV induces extensive cytopathic effects (CPE) specifically in tumor cells by intercellular fusion and syncytial formation while causing minimal damage in non-transformed cells. This selective oncolytic activity against human cancers has been mainly attributed to the elevated expression of CD46 on tumor cells [13]. An earlier phase I dose escalation clinical trial to test the safety of intraperitoneal administration of MV-CEA, a recombinant MV genetically modified to express a soluble marker peptide to enable non-invasive monitoring of the profiles of viral gene expression, was recently completed [14]. We observed that the virus was well tolerated, and no dose-limiting toxicity was observed. Although no dose-limiting toxicity was observed, there was development of anti-CEA antibodies and increase in anti-MV antibody titers [14]. Although replication-competent MV viruses can propagate selectively in tumor, the major limitation with systemic MV therapy for cancer remains the inefficiency of gene delivery to cancer cells *in vivo* due to host's immunity against MV. We are therefore keen to explore various strategies to improve delivery of measles virus to the tumor site, especially in patients with pre-existing anti-measles antibodies.

Mesenchymal stromal cells (MSC) are multipotent non-hematopoietic cells that can self-renew and exhibit ability to differentiate into multiple lineages with specific surface marker expression [15,16]. Many studies have demonstrated their remarkable tumor tropic and strong immunosuppressive properties [17,18]. Consequently, MSCs have been exploited in many clinical settings, including regenerative medicine, immune modulation, and tissue engineering. Accumulating pre-clinical and clinical studies have further demonstrated the efficacy of genetically modified MSC to express and release therapeutic factors, confirming their ability to serve as an excellent base for cell-mediated gene therapy.

In this study, we have evaluated the combination of the potent oncolytic activity of the attenuated MV against human tumors with the unique immunoprivileged and tumor-tropic biological properties of BM-hMSCs to combat human HCC, orthotopically implanted in SCID mice, passively immunized with human neutralizing antibodies against MV as a preclinical model.

Materials and methods

Cell cultures and viruses

All HCC cell lines and Vero cells were maintained in Dulbecco's modified Eagle's medium(DMEM) containing 10% and 5% fetal bovine serum, respectively. MV-expressing green fluorescent protein (GFP), firefly luciferase (FLuc), and sodium iodide symporter (NIS) were prepared as described previously [19]. These viruses exhibit comparable growth characteristics on Vero producer cells (Supplementary Fig. 1).

Isolation and characterization of human bone marrow-derived mesenchymal stem cells (BM-hMSCs)

This study was approved by the SingHealth Centralised Institutional Review Board (CIRB) and conducted in accordance with the policies of its Ethics Committee. Informed consent was obtained from all participating patients. BM-hMSCs were isolated and characterized as previously described [20]. Only low-passage cells (P4–P7) were used for all the experiments.

Virus infection assay

Cells were infected with MV-GFP at different multiplicities of infection (MOI) for 2 h at 37 °C. At the end of the incubation, virus inoculum was removed and the cells were maintained in culture medium containing fusion inhibitory peptide (FIP; Bachem, Germany). The percentage of GFP-positive infected cells was analyzed by flow cytometry. Cell viability was determined by MTS assay (Aqueous One Solution; Promega, WI). For cell heterofusion assays, green CFSE-stained (Invitrogen, CA) BM-hMSCs were infected with MV-FLuc (MOI = 2) and co-cultured with red Vybrant CM-DiI-labeled (Invitrogen) HuH7 cells. Cells were then maintained at 37 °C and cell heterofusion was observed under confocal microscopy (Carl Zeiss, Germany).

Plaque neutralization assay (PRN)

Pooled human AB sera were purchased from Valley Biomedical Inc. (Winchester, VA). Anti-measles antibody titers in pooled human sera were determined using anti-MV immunoglobulin (IgG) detection kit (Abnova, Taiwan). PRN assay was performed as described previously [21]. The numbers of plaques were counted at day 4 post-infection. Neutralizing titers were determined by the highest dilution of serum that resulted in at least 50% inhibition of cytopathic effect in at least two out of three wells. Anti-measles antibody titers are reported as EU/ml.

Orthotopic implantation of human hepatocellular carcinoma in SCID mice

Freshly resected human HCC tumors were collected from patients undergoing partial liver resection for HCC at the Singapore General Hospital. All samples were collected with informed consent and have been approved by SingHealth CIRB. Tumor tissues harvested were cut into small pieces and implanted subcutaneously into SCID mouse. When the tumor volume reached approximately 1 cm^3, tumor was harvested, cut into 1 mm^3 pieces and then implanted orthotopically into the liver of SCID mice. The development of tumor was monitored by measuring the serum levels of alpha-fetoprotein (AFP) using the human AFP ELISA detection kit (Abnova). At euthanasia, tumor size was measured using calipers.

In vivo experiments

All animal experiments were performed according to protocols approved by the SingHealth Institutional Animal Use and Care Committee. To determine the half-life of human anti-MV antibody post-passive transfer into SCID mice, SCID mice were given an i.p. injection of anti-measles serum, euthanized and bled at 3 h (day 0), day 1, 2, 3, 4, 5, and 6 post transfer. The level of anti-MV Ab in the recipient mice was determined by PRN assay.

For *in vivo* imaging experiments, BM-hMSCs were infected with an MV cocktail (MV-NIS and MV-Luc at 10:1), labeled with 10 μM DiR, and injected intravenously via the tail vein into tumor-bearing SCID mice. Localization of the MV-infected BM-hMSCs and the subsequent transfer of MV infection to tumors were monitored by fluorescence and bioluminescence and were quantified using the Xenogen IVIS system (Caliper Life Sciences, CA). MV infection in the tumor site was also confirmed by immune-histochemical staining for MV nucleoprotein (MV-N), as previously described [22].

For efficacy testing of experimental therapy, tumor-bearing mice were passively immunized by intraperitoneal (IP) injection of 95 EU of measles immune serum 3 h prior to therapy and thereafter 47.5 EU daily throughout the experiment. All mice were given single dose (2×10^6) of free-virus or MV-infected BM-hMSCs via tail vein. Mice were euthanized when the AFP reached 1000-fold compared to the level at starting therapy.

Statistical analysis

Analysis of variance (ANOVA) and *t*-test were used for statistical comparisons between groups (GraphPad Prism 5.0; GraphPad Software, CA). A $p < 0.05$ was considered statistically significant.

Results

Susceptibility of BM-hMSCs to MV infection

BM-hMSCs were infected with MV-GFP and infectivity was quantitated by flow cytometry. Increasing the MOI produced a corresponding increase in the numbers of infected cells (Fig. 1A), ranging from 40–45% for MOI of 1 to 60–72% for MOI of 4 at 96 h (Fig. 1B) with no significant effect on cell viability for up to 96 h post-infection (Fig. 1C).

In vitro transfer of MV infection from pre-infected BM-hMSCs to tumor cells via heterofusion

The ability of MV-infected BM-hMSCs to transfer the virus to human HCC cells was assessed in co-culture experiments using dual-fluorescent-labeled cells. Pre-infected green CFSE-stained BM-hMSCs were overlaid onto monolayer of red CM-DiI-labeled human HuH7 cells at 1:20 ratio. After co-cultured for 48 and 72 h, significant heterocellular fusion was observed (Fig. 1D) as evidenced by the formation of large multinucleated yellow syncytia resulting from the fusion of the red HuH7 cells and green MV-infected BM-hMSCs (Fig. 1Eii). By contrast, no heterofusion events were seen if uninfected BM-hMSCs were mixed with HuH7 cells (Fig. 1Ei). The extent of syncytia formation increases with the increasing number of MV-infected BM-hMSCs (Fig. 1F).

Experimental SCID mouse model for human hepatocellular carcinoma

We have developed an orthotopic model of human HCC by surgically implanting serially transplantable patient-derived HCC into SCID mice. All tumors grew locally in the liver (Fig. 2A). The serum AFP level correlated well with the tumor size ($R^2 = 0.9339$; $p = 0.01$; Fig. 2B). Mice (for example, #2–1), in which there was no macroscopic tumor detectable, also gave no detectable AFP (Fig. 2A and B). There was a latency period of approximately 2

weeks after which the AFP level (ng/ml) increased rapidly from 3404 ± 1348 (day 14) to 17,850 ± 12,020 (day 18) (Fig. 2C). Using these observations as reference, we employed mice with detectable AFP level ≥500 ng/ml, typically around 11 days post-tumor implantation (inset, Fig. 2C), for subsequent experiments.

MV-infected BM-hMSCs transferred MV infection to orthotopically implanted human HCC tumors and replicated in the HCC cells of the recipient SCID mouse

Targeting of MV-infected BM-hMSCs *in vivo* and the subsequent inhibition of tumor growth were demonstrated in the orthotopically implanted human HCC model. SCID mice bearing patient-derived HCC tissues or HuH7 tumors were given DiR-labeled MV-infected BM-hMSCs or cell-free viruses intravenously. MV mixture consisting of 1:10 MV-FLuc:MV-NIS was used in the experiment to enable *in vivo* monitoring of viral replication by imaging for FLuc expression as well as evaluating the efficacy of MV-NIS.

DiR signals (for monitoring BM-hMSCs) were detected in the livers of all the mice that received DiR-labeled MV-infected BM-hMSCs on day 2 post-cell infusion, but signal intensity faded by day 5 (Fig. 3A). At day 2 post-injection, weak FLuc signal could be detected in only one out of three mice bearing patient-derived HCC tumor and none in the mice implanted with HuH7 tumors that received MV-infected BM-hMSCs (Fig. 3A). However, the FLuc signals continued to increase with time, suggesting active viral replication. Furthermore, the FLuc signal overlapped with the DiR signal, indicating that it was possibly due to the transfer of MV infection from MV-infected BM-hMSCs to the orthotopically implanted HCC tumor cells. Moreover, both cell-free and hMSC-associated MV viruses were highly efficient in inhibiting the development of tumors in treated mice compared to control mice (Fig. 3B). Immunohistostaining of tumor cryosections was performed and measles nucleocapsid (MV-N) protein was detected in both cell-free virus and MV-infected BM-hMSCs-treated tumors, confirming the spread of MV viruses in the treated mice (Fig. 3C).

Cell-associated MV virus is more resistant to neutralizing anti-MV antibodies than cell-free MV virus

Cell-free MV-GFP or MV-GFP-infected BM-hMSCs were added to monolayer culture of Vero cells in the absence or presence of increasing concentrations of measles-immune serum (anti-MV IgG titer = 190 EU/ml). As shown in Fig. 4A, the virus infectivity recovered gradually with increasing dilutions of measles-immune sera. At 1:16 dilution, 30% of syncytia were present in Vero cells overlaid with MV-infected BM-hMSCs. In comparison, cell-free MV viruses were completely neutralized at this same serum dilution. For the cell-free MV viruses, only 15% of syncytia could be recovered in the Vero monolayer even at the serum dilution of 1:256 (Fig. 4A), indicating cell-associated viruses were more efficiently protected from the neutralizing effect of host anti-MV antibodies. Similar trends were observed in two additional independent experiments where at high concentration of measles-immune sera (up to 128-fold diluted), naked MV was less effective in inducing cell fusion compared to MV delivered in BM-hMSCs (Supplementary Fig. 2).

Cell-associated but not cell-free MV viruses suppressed HCC growth in the presence of measles immune serum

Mice are not susceptible to infection by measles virus because they lack the CD46 receptor required for virus entry. Measles virus is also unable to replicate in murine tissues due to an intracellular block of the transcription of viral genes [16,17]. Thus, we employed the passively immunization strategy in which human measles immune serum was injected IP into mice to produce measles immunity. The immune status of the recipient SCID mice was validated by measuring the level of neutralizing anti-MV antibodies present in their sera over time. At 3 h post-infusion, the mice were confirmed to be immune to measles with the half-life of passively acquired MV antibodies determined to be approximately 21.4 h (Fig. 4B).

The geometric mean antibody titers against measles in the sera of newly diagnosed HCC patients and healthy individuals are 169 ± 28.22 EU/ml (n = 8) and 117 ± 65.77 EU/ml (n = 4), respectively (Table 1). To test the effect of MV virotherapy with antibody treatment, tumor-bearing SCID mice were passively immunized with human measles immune serum at 20 EU/mouse (low) or 95 EU/mouse (high). Three hours later, all the passively immunized mice received one intravenous injection of 2×10^6 - $TCID_{50}$ MV cocktail (10 MV-NIS: 1 MV-FLuc) (n = 5 mice/group). Measles-naïve mice were also treated with the same amount of virus (n = 3 mice). No significant luciferase signals were detected in all the mice on day 1 after virus infusion (Fig. 4C). On day 3, there were intense signals in tumors of all measles-naïve mice and mice immunized with 20 EU immune sera. By contrast, luciferase signals detected in mice given 95 EU measles-immune sera were approximately 10-fold lower compared to both measles-naïve and 20 EU-immunized mice. Virus spread, indicated by quantification of intratumoral luciferase activity, in naïve mice and mice receiving 20 EU measles-immune serum, was comparable, but virus spread was significantly reduced in mice given 95 EU immune sera compared to the other two groups ($p < 0.05$; Fig. 4D). These observations further suggested that cell-free viruses were able to infect and spread to tumor cells in the presence of low (20 EU) but not high neutralizing anti-MV antibody (95 EU).

To determine if BM-hMSCs can deliver and protect MV in the presence of pre-existing immune serum, SCID mice bearing orthotopically implanted patient-derived HCC xenograft were passively immunized by IP injection of human measles immune serum (95 EU) or saline three hours pre-therapy. Mice were then treated intravenously either with 2×10^6 cell-free MV or 2×10^6 MV-infected BM-hMSCs cells. The BM-hMSCs were pre-infected with MV at MOI of 2. Quantification of serum AFP indicated that HCC developed progressively in saline-treated control mice, Fig. 4E. Cell-free MV viruses significantly suppressed tumor growth only in human measles immune serum naïve mice ($p < 0.01$) but not in measles-immune mice, Fig. 4E. Furthermore, there was a significant difference in therapy outcome for cell-free MV viruses in the presence or absence of human measles-immune serum ($p < 0.05$), Fig. 4E. On the other hand, treatment of both measles-naïve and measles-immune mice with MV-infected BM-hMSCs achieved good tumor control ($p < 0.01$ and $p < 0.05$, respectively), with no significant difference in therapy outcome between measles-naïve mice and mice receiving measles-immune sera (Fig. 4E), demonstrating that the presence of pre-existing measles-immune sera did not diminish the therapeutic efficacy of MV delivered in

BM-hMSCs. These results are further supported by the observations that tumor growth between the immune cell-free MV group and the control group was similar (Fig. 4E) while MV-infected BM-hMSCs immune mice achieved significant tumor suppression compared to the control group ($^{*}p < 0.05$), Fig. 4E.

Discussion

There are a number of challenges associated with intravenous administration of viruses that could limit the efficiency of measles virotherapy. Intravenously injected MV can be quickly neutralized by antimeasles antibodies in previously vaccinated individuals. Liver and spleen sequestration of viral particles also reduces the circulatory half-life of the virus and bioavailability to tumor cells. In addition, the virus has to extravasate efficiently from the lumenal side of tumor blood vessels into the tumor parenchyma to initiate an infection. We and others have suggested that cells infected with replication-competent MV viruses can serve as “Trojan horses” to deliver viruses to the tumor sites, alleviating virus sequestration and potential neutralization by the host immune factors.

In this study, we have firstly developed a highly reproducible model of human HCC in SCID mice. The spread of oncolytic viruses, which express the firefly luciferase reporter gene from the site of tumor inoculation, can be monitored using bioluminescent imaging for luciferase activity and this can be correlated with the tumor burden that can be quantitated by the measurement of AFP levels in the blood, since the orthotopically implanted HCC secreted AFP. Using this model, we evaluated and demonstrated the feasibility of using human MSC to deliver oncolytic MV to HCC orthotopically implanted in the liver of SCID mice that had been passively immunized against MV. Using DiR-labeled-MV-infected BM-hMSCs, we have demonstrated that MV-infected BM-hMSCs homed to orthotopically implanted HCC tumors, following systemic delivery via tail vein injection of tumor-bearing measles-immune SCID mice, and suppressed tumor growth. The average anti-MV IgG in newly diagnosed HCC patients has been estimated to be 169 EU/ml and is comparable to that of the healthy individuals (117 EU/ml). We maintained the anti-MV titer at 95 EU/mouse in our experiments and represented the maximum achievable antibody titer with the human measles-immune serum available in the lab. Although this was below the average observable anti-MV titer in HCC patients, this level was shown to produce sufficient inhibition of *in vivo* free virus replication and spread (Fig. 4C and D) and is also significantly higher than the titer of 20 EU/ml, at which an individual is considered to be measles immune.

There is, however, another set of potential challenges associated with the use of cells as carriers for virotherapy. We and others have previously shown that systemically administered cell carriers tend to arrest in the lungs, immediately upon infusion and could diminish the efficacy of cell-mediated virotherapy [23,24]. However, we have subsequently demonstrated that CD14 monocytes, immature dendritic cells, interleukin-2 expanded T cells arrested in lungs are only transient and they are later disseminated to the liver, spleen, and bone marrow after the initial arrest [25,26]. The pattern of transient cell arrest in the lungs and subsequent redistribution to liver and spleen was also seen in human studies where ^{111}Indium oxine-labeled peripheral blood lymphocytes or T cells were injected

intravenously into humans and monitored using gamma cameras [27]. As with other non-transformed cells, it requires a large amount of MV to infect significant numbers of BM-hMSCs carriers (Fig. 1B, 60% infectivity at MOI = 4). Moreover, virus replication/progeny production was 10-fold less in Vero monolayer cells infected with the same amount of MV-infected BM-hMSCs compared to infection with free virus (data not shown).

However, using MSC as a carrier for HCC therapy offers many attractive features. Circulating MSC cells can home to the liver and the trafficking profiles of MSC cells are well studied. In addition to its natural tropism for the tumor, MSC can efficiently be infected by MV, as well as support viral gene expression. Many thorough safety studies using high numbers of MSC have been reported and employed for clinical studies [10]. The human experience, together with the extensive toxicology and pharmacology studies, has demonstrated the safety of using MSC cells in patients with end stage cancer, making the strategy of cell carriers highly feasible for clinical testing. Currently, MSC based clinical trials have been conducted for at least 12 kinds of pathological conditions, with many completed trials demonstrating safety and efficacy [10]. In addition, there are further compelling reasons to use cell carriers for systemic delivery of MV. Unlike “naked” MV, which can be rapidly sequestered by the reticuloendothelial system or neutralized by antiviral antibodies in the circulation, we have demonstrated here that cell-associated MVs are protected from antiviral antibodies (Fig. 4A). Subsequent virus transfer via heterocellular fusion between infected cell carriers with target cells is more resistant to neutralization by anti-MV antibodies, perhaps because the interface of cell-to-cell fusion is less accessible to antibodies than the junction of virus-cell membrane fusion. Indeed, MV may be particularly suited for cell carrier delivery as natural MV infection is cell-associated [28].

Supplementary Material

Refer to Web version on PubMed Central for supplementary material.

Acknowledgments

The technical support of Amudha Deivasigamani is greatly appreciated.

Financial support

This work was supported by grants from the National Medical Research Council, Biomedical Research Council of Singapore, The Singapore Millennium Foundation and the SingHealth Foundation.

References

1. Ferlay J, Shin HR, Bray F, Forman D, Mathers C, Parkin DM. Estimates of worldwide burden of cancer in 2008: GLOBOCAN 2008. Int J Cancer. 2008; 127:2893–2917. [PubMed: 21351269]
2. El-Serag HB, Rudolph KL. Hepatocellular carcinoma: epidemiology and molecular carcinogenesis. Gastroenterology. 2007; 132:2557–2576. [PubMed: 17570226]
3. Farazi PA, DePinho RA. Hepatocellular carcinoma pathogenesis: from genes to environment. Nat Rev Cancer. 2006; 6:674–687. [PubMed: 16929323]
4. Bruix J, Sherman M. Management of hepatocellular carcinoma: an update. Hepatology. 2011; 53:1020–1022. [PubMed: 21374666]

5. Clavien PA, Lesurtel M, Bossuyt PM, Gores GJ, Langer B, Perrier A. Recommendations for liver transplantation for hepatocellular carcinoma: an international consensus conference report. Lancet Oncol. 2012; 13:e11–e22. [PubMed: 22047762]
6. Zarrinpar A, Kaldas F, Busuttil RW. Liver transplantation for hepatocellular carcinoma: an update. Hepatobiliary Pancreat Dis Int. 2011; 10:234–242. [PubMed: 21669564]
7. Burrel M, Reig M, Forner A, Barrufet M, de Lope CR, Tremosini S, et al. Survival of patients with hepatocellular carcinoma treated by transarterial chemoembolisation (TACE) using Drug Eluting Beads. Implications for clinical practice and trial design. J Hepatol. 2012; 56:1330–1335. [PubMed: 22314428]
8. Bruix J, Raoul JL, Sherman M, Mazzaferro V, Bolondi L, Craxi A, et al. Efficacy and safety of sorafenib in patients with advanced hepatocellular carcinoma: subanalyses of a phase III trial. J Hepatol. 2012; 57:821–829. [PubMed: 22727733]
9. Llovet JM, Ricci S, Mazzaferro V, Hilgard P, Gane E, Blanc JF, et al. Sorafenib in advanced hepatocellular carcinoma. N Engl J Med. 2008; 359:378–390. [PubMed: 18650514]
10. Russell SJ, Peng KW, Bell JC. Oncolytic virotherapy. Nat Biotechnol. 2012; 30:658–670. [PubMed: 22781695]
11. Blechacz B, Splinter PL, Greiner S, Myers R, Peng KW, Federspiel MJ, et al. Engineered measles virus as a novel oncolytic viral therapy system for hepatocellular carcinoma. Hepatology. 2006; 44:1465–1477. [PubMed: 17133484]
12. Russell SJ, Peng KW. Measles virus for cancer therapy. Curr Top Microbiol Immunol. 2009; 330:213–241. [PubMed: 19203112]
13. Ong HT, Timm MM, Greipp PR, Witzig TE, Dispenzieri A, Russell SJ, et al. Oncolytic measles virus targets high CD46 expression on multiple myeloma cells. Exp Hematol. 2006; 34:713–720. [PubMed: 16728275]
14. Galanis E, Hartmann LC, Cliby WA, Long HJ, Peethambaram PP, Barrette BA, et al. Phase I trial of intraperitoneal administration of an oncolytic measles virus strain engineered to express carcinoembryonic antigen for recurrent ovarian cancer. Cancer Res. 2010; 70:875–882. [PubMed: 20103634]
15. Dominici M, Le Blanc K, Mueller I, Slaper-Cortenbach I, Marini F, Krause D, et al. Minimal criteria for defining multipotent mesenchymal stromal cells. The International Society for Cellular Therapy position statement. Cytotherapy. 2006; 8:315–317. [PubMed: 16923606]
16. Pittenger MF, Mackay AM, Beck SC, Jaiswal RK, Douglas R, Mosca JD, et al. Multilineage potential of adult human mesenchymal stem cells. Science. 1999; 284:143–147. [PubMed: 10102814]
17. Jones BJ, McTaggart SJ. Immunosuppression by mesenchymal stromal cells: from culture to clinic. Exp Hematol. 2008; 36:733–741. [PubMed: 18474304]
18. Reagan MR, Kaplan DL. Concise review: Mesenchymal stem cell tumor-homing: detection methods in disease model systems. Stem Cells. 2011; 29:920–927. [PubMed: 21557390]
19. Peng KW, Facteau S, Wegman T, O'Kane D, Russell SJ. Non-invasive in vivo monitoring of trackable viruses expressing soluble marker peptides. Nat Med. 2002; 8:527–531. [PubMed: 11984600]
20. Ho IA, Toh HC, Ng WH, Teo YL, Guo CM, Hui KM, et al. Human bone marrow-derived mesenchymal stem cells suppress human glioma growth through inhibition of angiogenesis. Stem Cells. 2013; 31:146–155. [PubMed: 23034897]
21. Ratnam S, Gadag V, West R, Burris J, Oates E, Stead F, et al. Comparison of commercial enzyme immunoassay kits with plaque reduction neutralization test for detection of measles virus antibody. J Clin Microbiol. 1995; 33:811–815. [PubMed: 7790442]
22. Mader EK, Maeyama Y, Lin Y, Butler GW, Russell HM, Galanis E, et al. Mesenchymal stem cell carriers protect oncolytic measles viruses from antibody neutralization in an orthotopic ovarian cancer therapy model. Clin Cancer Res. 2009; 15:7246–7255. [PubMed: 19934299]
23. Kidd S, Spaeth E, Dembinski JL, Dietrich M, Watson K, Klopp A, et al. Direct evidence of mesenchymal stem cell tropism for tumor and wounding microenvironments using in vivo bioluminescent imaging. Stem Cells. 2009; 27:2614–2623. [PubMed: 19650040]

24. Munguia A, Ota T, Miest T, Russell SJ. Cell carriers to deliver oncolytic viruses to sites of myeloma tumor growth. Gene Ther. 2008; 15:797–806. [PubMed: 18356812]

25. Ong HT, Hasegawa K, Dietz AB, Russell SJ, Peng KW. Evaluation of T cells as carriers for systemic measles virotherapy in the presence of antiviral antibodies. Gene Ther. 2007; 14:324–333. [PubMed: 17051248]

26. Peng KW, Dogan A, Vrana J, Liu C, Ong HT, Kumar S, et al. Tumor-associated macrophages infiltrate plasmacytomas and can serve as cell carriers for oncolytic measles virotherapy of disseminated myeloma. Am J Hematol. 2009; 84:401–407. [PubMed: 19507209]

27. Read EJ, Keenan AM, Carter CS, Yolles PS, Davey RJ. In vivo traffic of indium-111-oxine labeled human lymphocytes collected by automated apheresis. J Nucl Med. 1990; 31:999–1006. [PubMed: 2112185]

28. Esolen LM, Ward BJ, Moench TR, Griffin DE. Infection of monocytes during measles. J Infect Dis. 1993; 168:47–52. [PubMed: 8515132]

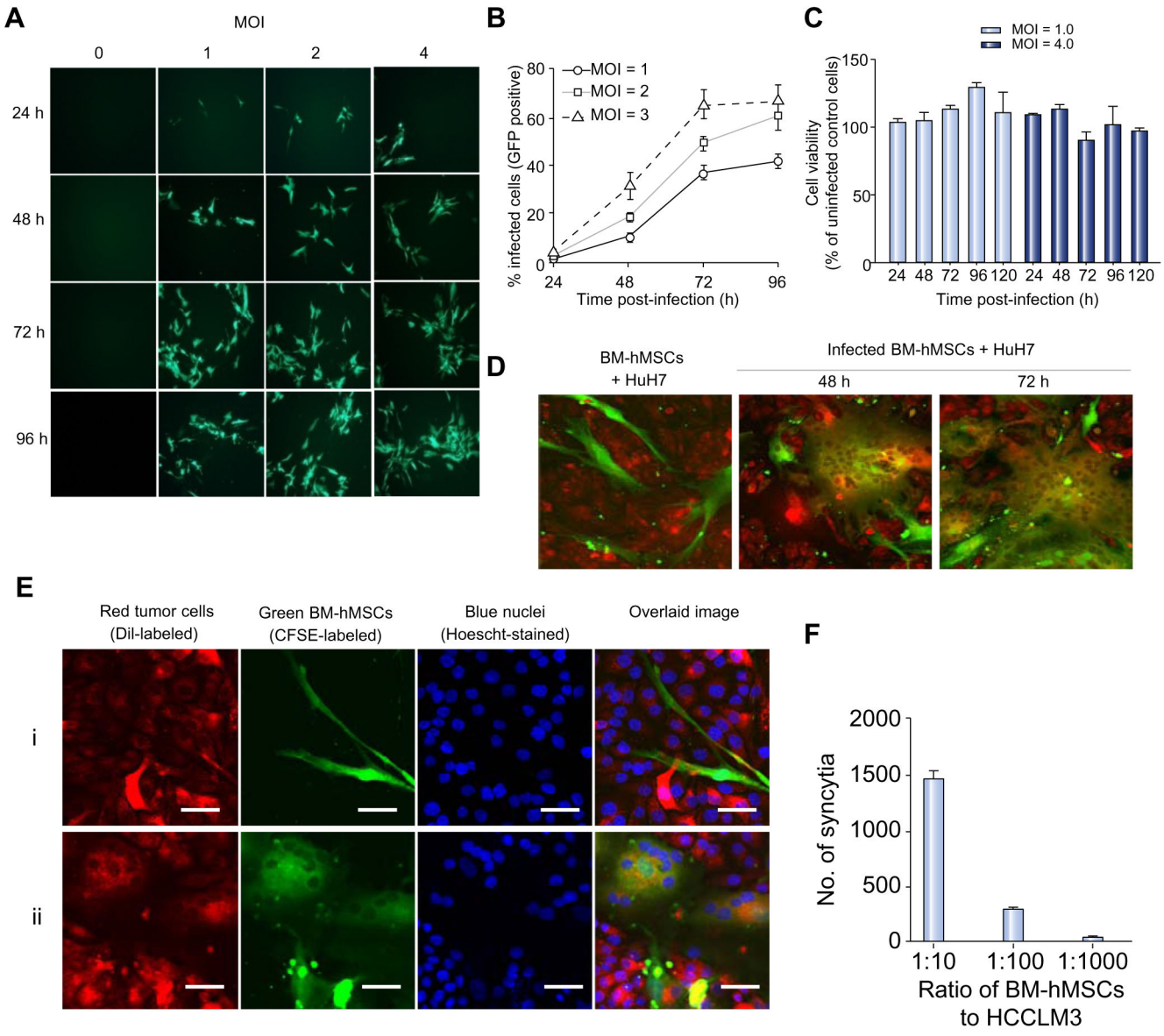

Fig. 1. MV can infect BM-hMSCs and transfer the infection to HCC cells *in vitro*

(A) BM-hMSCs were infected with MV-GFP, (B) quantitated by flow cytometry for GFP-expressing cells and (C) evaluated for cell viability with MTS assay at the indicated time-points. CFSE-stained MV-infected BM-hMSCs were overlaid on DiI-labeled HuH7 cells at a 1:20 ratio. (D) At 48 and 72 hours post-overlaid, cells were photographed with a confocal microscope. (E) High-resolution analysis of heterofusion between green BM-hMSCs and red HuH7 cells resulted in observation of multinucleated yellow-colored synctia (Eii). For comparison, co-culture of uninfected BM-hMSCs (green) with HuH7 (red) did not result in heterofusion (Ei). Scale bar = 50 μm. (F) MV-induced syncytia formation increases with the number of infected BM-hMSCs. (This figure appears in colour on the web.)

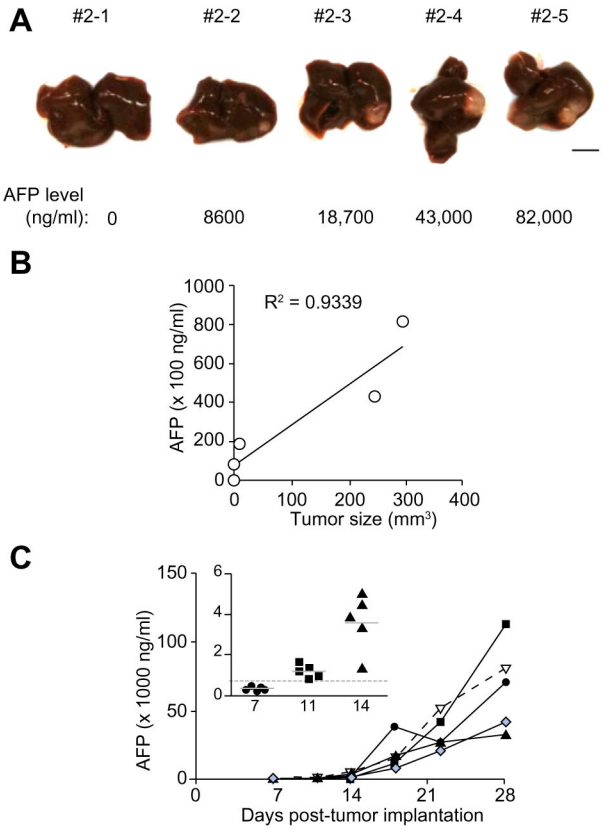

Fig. 2. Orthotopically implanted human HCC tumor model

HCC tumors were surgically implanted into the liver of SCID mice. (A) Macroscopic view of the implanted tumor developed in the liver of a representative SCID mouse with their corresponding serum AFP level indicated below the picture. Scale bar = 5 mm. (B) AFP levels plotted against tumor size. $R^2 = 0.9339$ and $p = 0.01$. (C) Growth kinetics of the orthotopically implanted HCC tumor. Tumor growth increased rapidly when serum AFP level was >500 ng/ml, indicated by the dotted line (in the inset). (This figure appears in colour on the web.)

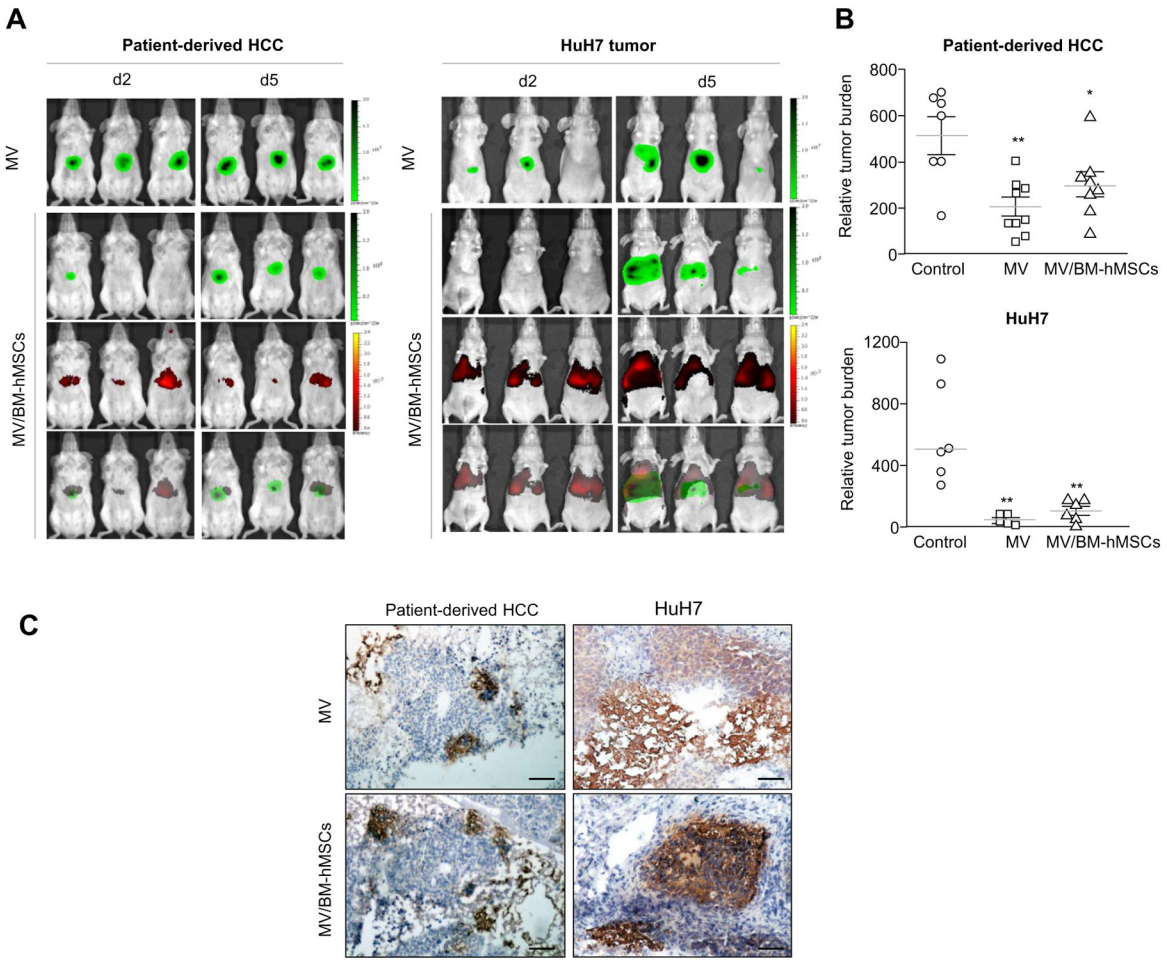

Fig. 3. Systemic delivery of MV infection via infected BM-hMSCs to orthotopically implanted HCC tumors resulted in significant tumor growth suppression

(A) Tumor-bearing mice were given 2×10^6 $TCID_{50}$ MV-Luc or 2×10^6 MV-Luc-infected DiR-labeled BM-hMSCs (MV/BM-hMSCs). Bioluminescence imaging of virally encoded firefly luciferase is shown in green, and fluorescence imaging of DiR-labeled BM-hMSCs is indicated in red. Overlaid images (bottom panel) showed colocalization of both signals indicating delivery of MV-Luc infection (green) by infected BM-hMSCs (red). (B) Relative tumor burden at necropsy; $^{**}p < 0.01$; $^{*}p < 0.05$. (C) Immunohistochemistry staining for MV-N protein. Scale bar = 50 μm. (This figure appears in colour on the web.)

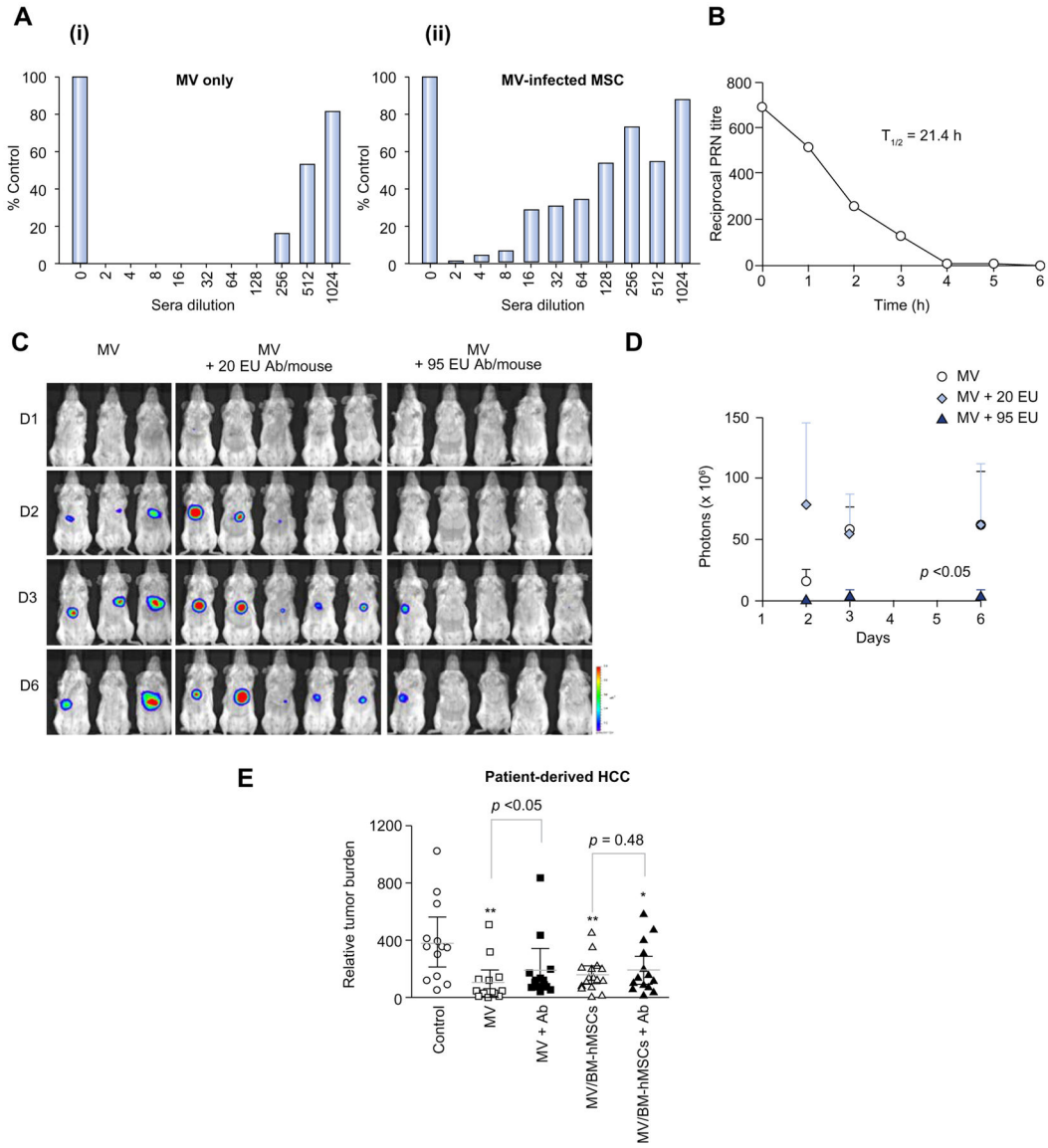

Fig. 4. BM-hMSCs protect MV from anti-MV neutralization

(A) The degree of *in vitro* MV infection by cell-free or cell-associated MV after exposure to increasing dilutions of measles-immune serum is represented as a percentage of syncytia count in the absence of anti-MV serum. (B) Timeline for decay of human measles-immune serum in SCID mice. (C) Bioluminescence imaging of viral spread in low and high anti-MV antibodies, (D) quantitated in photon counts. (E) Relative tumor burden in measles-naïve and passively immunized tumor-bearing mice treated with cell-free or cell-associated MV via intravenous injection; $^{**}p < 0.01$; $^{*}p < 0.05$. (This figure appears in colour on the web.)

Table 1

Anti-MV IgG levels in newly diagnosed HCC patients and healthy donors.

Sample ID	Anti-MV IgG (EU/ml)
HCC patients	
240T	177.43
239T	169.89
234T	189.69
233T	192.47
232T	171.42
231T	195.21
196245	113.81
196140	140.98
Healthy donors	
1	76.46
2	180.41
3	145.50
4	163.90